Plane Wave Imager

A note to the reader.

A Plane Wave Imager (PWI) replaces the lens with an array of evanescent couplers. PWI forms an image using the same light characteristics as a lens. Unlike a lens, the optical path length in silicon can be controlled by varying current in an implanted diode. No attempt is made to keep optical path lengths equal. Rather, during data collection, the path length difference between coupler arms is swept (varied), and the mean signal recorded. For reasons explained in this paper, real-time uniformity correction is easy to implement. Far from being impossible or impractical, PWI implementation should be straightforward.

1. Introduction

Plane Wave Imagers (PWI) are flat plates that form images of incoherent light by measuring the angle of arrival of light impinging on their surface. Further, large apertures can be created by combining the digital data from many small PWI without precise pre-alignment of the sub-imagers. Figure 1 illustrates how a large optical aperture is formed by assembling an array of small PWI. The procedure for combining data from many PWI to generate a high resolution image is described in a later section of this paper.

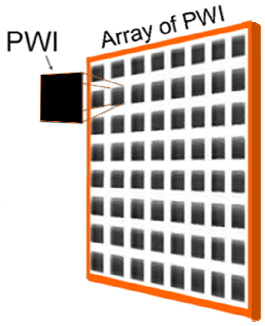

Figure 1. Individual PWI are represented by the small black squares. The array of PWI creates a large effective aperture with image resolution up to eight times that of a single PWI.

Because PWI operate directly on plane waves of light, image resolution for an individual PWI is near theoretical limits. When assembling large apertures using many small PWI, some degradation of image resolution does occur if the several sub-imagers are not perfectly aligned. However, digital processing of the PWI data can make the degradation is surprisingly small. For example, if the optical axes are misaligned by a tenth of the field of view, both resolution and field of view degrade (decrease) by ten per cent.

As explained in a later section of this paper, the theoretical limit for thermal PWI noise equivalent temperature is an order of magnitude lower (better than) lensed imagers. For reflective imagery, signal to noise and contrast limitations are about the same. Another performance advantage is that PWI focus is digital. In most respects, focus behavior very much resembles that of ordinary cameras, except PWI focus is easier to correct.

Further, PWI can be fabricated in CMOS foundries. PWI uses technology developed by researchers interested in communications applications, but their work directly applies to imaging. Recognizing the need for economy in the competitive communications market, the researchers

used only processes that are commonly available in silicon foundries. Further, the area of an individual PWI is about a square inch, a size that is considered economically producible in CMOS.

Section 2 will summarize PWI operation and hopefully provide a convincing argument that PWI is not only feasible but actually practical. Later sections of the paper will provide details.

2. A Brief Explanation of Plane Wave Imager Theory

This section covers two topics. The first topic is a description of how PWI images incoherent light. Later sections of this paper provide additional details on signal collection, signal processing, and non-uniformity correction. This section describes concept and not details.

The second topic is a discussion on how multiple PWI images are combined to improve spatial resolution of the scene. The several PWI must gather data near-simultaneously, but the several imagers need not be precisely spatially aligned.

Incoherent Imaging:

In Figure 2, A represents a train of light waves. The Poynting Vector indicates direction of travel. The plane waves shown perpendicular to the Poynting Vector are surfaces of constant phase of the electric (E) field. In B, light leaves an emission point and expands as a spherical surface. The PWI is far enough away from the emission point that the constant phase surfaces are essentially flat planes upon arrival. By "constant" phase, we mean that when one plane wave of light encounters a plane surface parallel to that wave (that is, normal to the Poynting Vector), the E field in that parallel plane points in one direction. At all points on that parallel surface, the E field is changing rapidly but in unison.

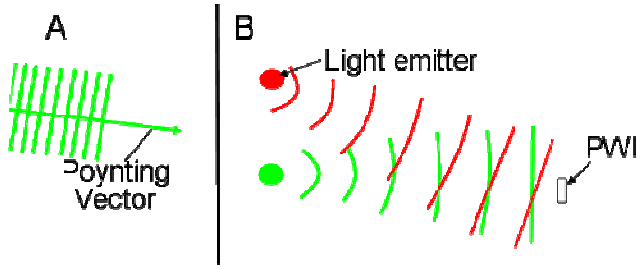

Figure 2. In A, the Poynting Vector indicates the direction of travel of light. In this paper, we typically show surfaces of constant phase instead. In B, light becomes planar as it spreads out from the emission point.

In Figure 3A, the light is parallel to the PWI surface, and in B the light enters at an angle. The spatial frequency and direction of the phase pattern on the PWI surface depends upon the angle of arrival of the light waves. Figure 4 shows one pattern for light at angle ϕ. Note that light from different emission points does not cross-correlate. Further, light from the same emission point correlates with itself, but when a sequence of waves arrives at a non-zero angle, then different waves intersect the PWI surface at any one instant in time. In that case, light hitting different points on the PWI surface will not correlate at full intensity.

Figure 5 shows a Michelson Interferometer. Arrows and lines with slightly different colors and patterns have been added to help track the light paths. Shifting the movable mirror results in the

intensity plot shown at right in the figure. Incoherent light forms interference fringes when split and re-combined with near-zero delay between the split light streams. For this particular plot, the light correlation length is based on a 4 micron mean wavelength and a 0.4 micron spectral bandwidth.

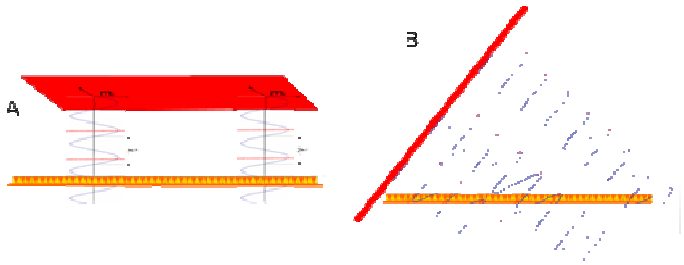

Figure 3. At left, the plane wave in A is parallel to the PWI surface (the Poynting Vector is normal) and light in neighboring PWI light collection sites is in phase. In B, the phase between light entering adjacent light collection sites varies.

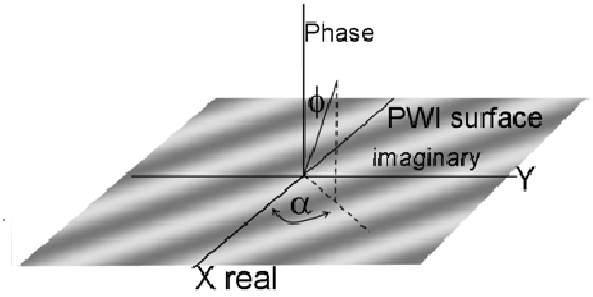

Figure 4. The pattern in the figure represents the phase at intersection with the PWI surface.

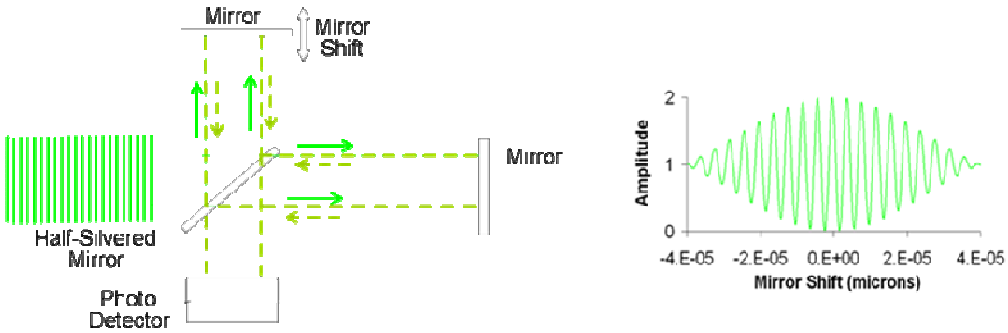

Figure 5 showing an interferometer and fringe interference of incoherent light.

In Figure 6, the modified interferometer superimposes different areas of the plane wave surface, and the same interference intensity behavior occurs as in Figure 5.

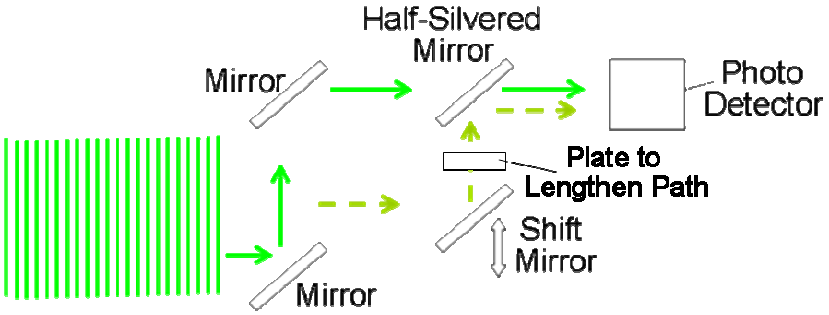

Figure 6 illustrates what would happen if different portions of the same plane wave were superimposed. The resulting fringe intensities would be the same as the plot in Figure 4.

Consider the following two points. First, a lens works because the E field (H field) vectors across the plane wave (perpendicular to the Poynting Vector) point in the same direction at any one instant in time. That occurs because the plane wave is formed by light spreading from a single source. Second, light from diverse points in the scene does not exhibit cross-coherence. Those two points are true when imaging with a lens, and they are equally true when imaging using evanescent couplers etched into a photonics array.

Consider a one dimensional example using light with wavelength λ entering the PWI at angle ϕ. The PWI unit cells have pitch d and the array length is L. Adjacent unit cells see a phase difference ($\Delta\theta$) of

$$\Delta\theta = \frac{2\pi \sin(\phi)\, d}{\lambda} \tag{1}$$

With uniformly spaced unit cells, angle ambiguity occurs at an angle ϕ_a

$$\phi_a = \pm \sin^{-1}\left(\frac{\lambda}{d}\right) \tag{2}$$

That is, a PWI imager has side lobes, meaning that light arriving at an angle ϕ bigger than ϕ_a is imaged at MOD(ϕ - ϕ_a) where MOD is the modulus function.

In Figure 4, the Poynting Vector of a plane wave makes an angle ϕ with the Z axis of a Cartesian coordinate system where the XY plane is the surface of the PWI. The angular position of the point source in space that generates the plane wave is given by the angles (α,ϕ) as defined in Figure 4. Equation 3 gives the phase of the plane waves at locations X = Nd and Y = Md.

$$f^{X}_{PWI}(\phi,\alpha) = \frac{2\pi N\, d \cos(\alpha)\sin(\phi)}{\lambda}$$

$$f^{Y}_{PWI}(\phi,\alpha) = \frac{2\pi M\, d \sin(\alpha)\sin(\phi)}{\lambda} \tag{3}$$

$$\text{E field(X,Y)} = A_{xy} \sin\left(f^{X}_{PWI}(\phi,\alpha) + f^{Y}_{PWI}(\phi,\alpha) + \beta\right)$$

The orientation and spatial period of the pattern formed on the PWI surface by the plane wave depends upon ϕ and α. There are many points in the scene reflecting or emitting light, each creating a different pattern. Different ϕ form different frequency patterns and different α change the orientation.

Light enters PWI via an array of small antenna horns or optical couplers spaced ten to thirty or forty microns apart on the PWI surface. The light in adjacent PWI waveguides gets its properties from the same combination of plane waves impinging on the whole PWI, but at slightly different locations and slightly different times and phases. The light in adjacent waveguides will exhibit the cross-correlation property illustrated in Figures 4 and 5, and that cross-correlation behavior will be established by the way that arriving individual plane waves sum at the different points on the PWI surface.

Figure 7 shows one concept for a light collection site (LCS). Item 1 couples light from the scene into a polarization diversifier (2). Item 2 converts all scene light to one mode compatible with the waveguide. Half the light is directed by splitter item 3 for processing in the neighboring LCS. Item 4 is an evanescent coupler (EC) and item 5 is a PIN diode implant in both of the EC arms; the diodes are used to adjust phase of the light entering the splitter/coupler. Item 6 controls diode current. Item 7 is two photo detectors configured to measure the difference signal out of the EC..

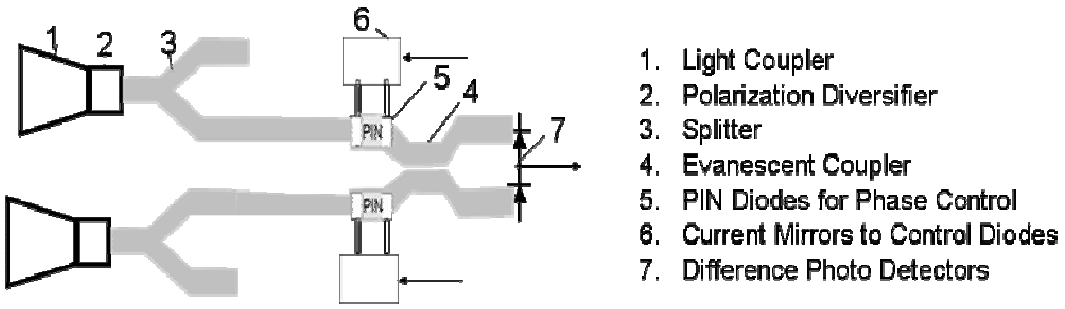

Figure 7. One concept for a light collection site or pixel.

Phase control diodes 5 are implanted on both sides of the EC. One function of the diodes is to use signals collected over several frames to keep the path lengths as close as practical. Another function of the diodes is to temporally modulate the path length during data collection. The diodes must be capable of varying optical path length over tens of wavelengths, so that light from adjacent couplers passes from zero correlation to peak and back to zero.

It is true that the same light arrives at all points on the PWI surface. However, the angular distribution of light results in the interference fringes from each emission contributor summing in a different manner over the PWI surface. Light from different emission points does not cause interference fringes, and the interference fringes arising from light incident at any particular angle will vary in a known way over the PWI area. Sensing the mean or peak amplitude of the interference fringes across the PWI surface provides the data needed to form an image.

Combining Poorly Aligned PWI Images to Improve Scene Resolution

Well-corrected lenses are diffraction limited. That is, spatial detail in the scene beyond the diffraction limited frequency is not present on the photo detector array. The high spatial frequencies have not be blocked by the optical aperture. Rather, diffraction blur is such that image contrast disappears beyond a certain frequency limit. The signal energy is there, but the modulation has disappeared.

It is well established that overcoming the diffraction limit requires using a large optical aperture. The large aperture can be accomplished by combining multiple small apertures. For example, the

technique employed in the famous Michelson-Morley Experiment. However, those optical apertures needed to be precisely aligned. After all, the signal cannot be recovered if it is not there. In an lensed imager that uses a small lens, the high spatial frequency modulation is not there.

PWI does not suffer aperture diffraction, but the resolution limits are exactly the same, numerically, as for aperture diffraction. With PWI, pitch establishes field of view. For example, a 4 micron imager using a 25 micron pitch would have a 9.2 degree field of view regardless of PWI size. A Larger PWI provides more pixels and better spatial resolution, but more pixels on the same array size simply increases field of view at the same resolution. Whatever size is selected for PWI, the PWI frequency limit exactly matches the lens aperture diffraction cutoff for that size.

However, what is to stop us from placing one, two, three, or twenty PWI beside the first? Each PWI collects independent samples from a slightly different spatial orientation than the others. The PWI are not spaced widely apart, because that would create a sparse aperture and poor imagery. But if the PWI are closely spaced, then digital processing can be used to align the images sub-pixel, and then we combine the digital data into a large array for a Discrete Fourier Transform using pixels from many PWI arrays.

The difference between processing multiple lensed apertures and processing multiple PWI, is that the high spatial frequencies are not present in any of the lensed images. With PWI, the additional imagers extend the angle measurement arm in the same way as fabricating a large area PWI.

3. Data Collection and Nonuniformity Correction.

During data collection, the PIN diodes are used to make the optical path lengths unequal in one direction, and then the path delays are swept through zero path difference to unequal in the other direction. The amplitude of the modulation shown in the plot at right in Figure 5 is recorded. That relatively simple procedure leaves us with two problems, however.

The first problem is that, while it is certainly possible to design light collection site electronics that determines which cell signal leads and which lags, that complicates PWI design. The second problem is that there are many ways for the gain of every site to vary. Splitters might not be perfect, waveguides might have different losses, light couplers and polarization diversifiers might be slightly different. Further, many of these nonuniformity factors vary with PWI temperature and age. A factory calibration is not sufficient.

The modified light collection site shown in Figure 8 solves both problems, although the modified design doubles data rate. By collecting the signals from both photo detectors, we know which leads and which lags. Further, we can now take both the sum and difference. The sum should always be equal across all the data, so variations in the sum provide gain correction for the current image frame.

To summarize:

- PWI implementation depends on the cross-correlation properties of incoherent light and not on the instantaneous phase of the light. At no point do we expect to maintain the

optical path lengths equal within a wavelength. We do expect that path length can be temporally modulated from zero modulation through maximum and back to zero.

- Differences across the PWI array due to dimensional tolerances, material variations, and temperature gradients are expected and handled by the PWI light collection site design.

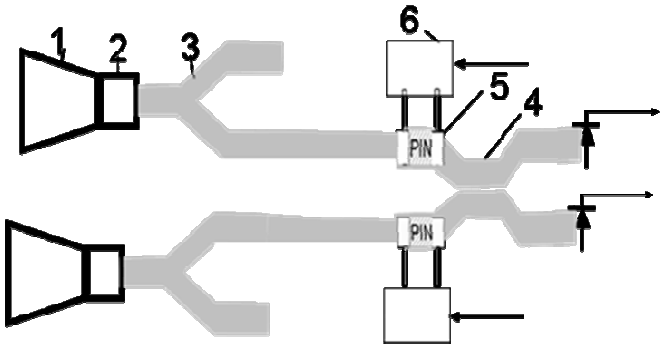

Figure 8. Figure 7 is modified to read the signal from both photo diodes.

4. Establishing Field of View and Field of Regard.

Field of view (FOV) is the solid angle viewed by a single PWI array; see Figure 9A. Field of regard (FOR) is the FOV of the whole array of PWI as illustrated in Figure 9B. An array of PWI can either cover a large FOV as in 9B or, by pointing all PWI in the same direction, the array can provide high resolution of a small FOV as illustrated by 9C.

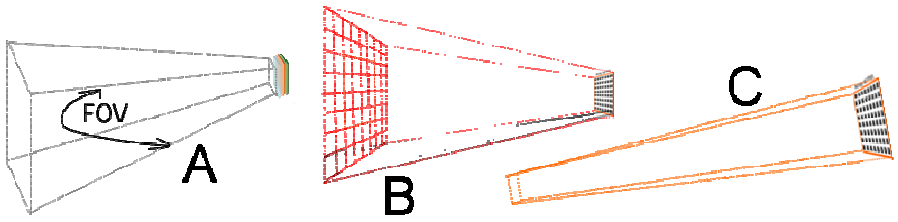

Figure 9 illustrates field of view (FOV) and field or regard (FOR).

The maximum resolution provided by an array of PWI is not based on dimension W in Figure 10. Rather, maximum resolution is determined by summing the dimension U of all PWI along a row or column of the array. Further, a wide FOV cannot be established by digitally processing data between arrays. The idea that the individual PWI in the array need not be uniformly spaced, or that the phases in each PWI can be electronically manipulated, is true, but expecting an array of PWI to act like a phased array radar is not realistic for a number of practical reasons. The wavelengths are just too small considering realistic dimensional tolerances.

One option for varying FOV and FOR is to add a liquid crystal phase plate in front of the PWI; see Figure 11. The phase plate would have a separate region for each individual PWI.

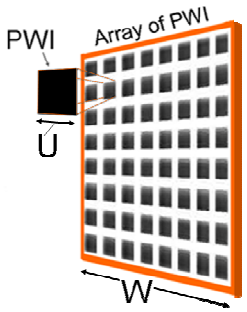

Figure 10 illustrating the dimension U that determines maximum resolution possible from the array of PWI. Dimension W is not it!

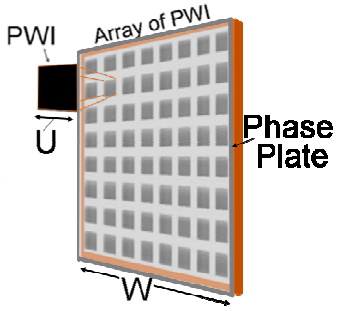

Figure 11. A liquid crystal phase plate might be added in front of the PWI array in order to point the individual PWI in different directions over time.

5. PWI Focus Behavior

Several worries about PWI focus have been addressed using computer simulations. The first worry was that nearby objects might obscure far objects even when not blocking the far object line-of-sight. That is not the case. Figure 12 has three rows of pictures. The top row outlines the portion of the PWI FOV shown in the bottom two rows. As range increases, the blur becomes too small to see if the whole FOV is shown at long range. The second row of pictures shows the focus blur; that is, PWI processing is set for infinity focus, and the blur shown results from a point source radiator placed at the range indicated. The bottom row shows the phase pattern on the PWI.

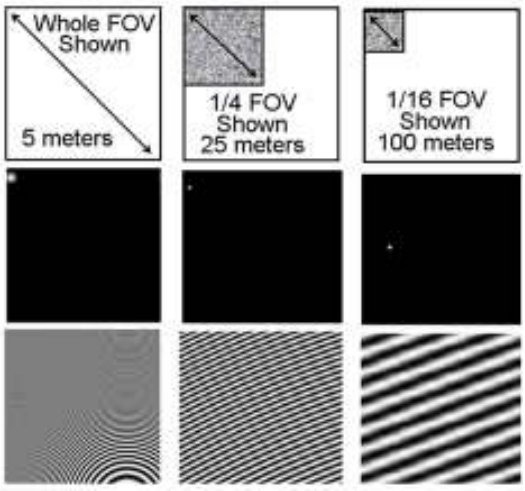

Figure 12. Focus blurs at three ranges.

The first and most important conclusion to be drawn from these pictures is that focus blur is localized, and looks very much the same as blur caused by lens defocus. Near objects do not generate spurious image content that obscures far objects. That is not really a surprise, but the worry had to be checked.

Secondly, and also not a surprise, blur is linear and spatially invariant. Therefore, focus blur is correctable digitally. The third worry was that infinity focus might be at or near infinity. Infinity focus is at about 250 meters for a 3 degree FOV, and that again mimics the blur behavior of lenses.

6. Plane Wave Imager Signal to Noise

PWI provides several signal to noise advantages over lensed imaging. This section only applies to passive imaging.

Signal:

The signals in each lensed pixel or PWI light collection site are equal provided the lensed optical aperture is the same size as the PWI array. In the lensed camera, all of the light from a point in space is focused onto one detector, but that detector has a small instantaneous FOV. In PWI, the light is spread across all LCS, but each LCS has an instantaneous FOV equal to the whole FOV. The signals are therefore equal.

However, the comparison in the last paragraph does not describe most of the performance trades that must be made when designing optical imagers. While we might suggest that large lens apertures can be replaced by an array of PWI, that begs the question as to whether the signals from each PWI have sufficient signal to noise to support the digital processing required to combine the imagery. Instead of equating aperture size of lensed and PWI, we now equate focal plane array size.

Equations 4 and 5 ignore optical transmission and other factors that will affect any type of imager. In the equations, A_d is the focal plane array (FPA) size, and the detector or LCS arrays have N horizontal and N vertical pixels. So the arrays have N^2 pixels covering a FPA area A_d. E_{sc} is scene radiance in watts per square centimeter. S_{lens} is lens signal per detector, S_{PWI} is PWI signal per LCS, and the lensed systems have F/1 optics.

$$S_{lens} = \frac{E_{sc}\, A_d}{4\, N^2} \tag{4}$$

The origin is Equation 4 is well known; see page 216 of the Burle Electro-Optics Handbook. S_{lens} is not range dependent because more and more scene is viewed by each detector as range increases.

A similar thing happens with a PWI, because more and more signal is added to the finite number of Fourier Transform frequency buckets as range increases. Both types of imager collect signal based on the instantaneous FOV of a pixel, and neither imager has a range-dependent signal.

$$S_{PWI} = \frac{E_{sc}\, A_d}{N^2} \tag{5}$$

We conclude that detector signals are essentially the same for lensed and PWI when lensed aperture equals PWI area or when lensed FPA area equals PWI area.

Three additional factors favor PWI performance over lensed designs. First, for thermal imagers, the E_{sc} in Equations 4 and 5 are not the same. For lensed systems, E_{sc} is the standard deviation resulting from changes across the scene. In that case, E_{sc} ranges from 0.1 to perhaps 20 Kelvins representing very poor to very good scene thermal contrast. In Equation 5, E_{sc} actually is the scene thermal emission, typically assumed to be 300 Kelvins. The theoretical performance of PWI thermal imagers far exceeds that of lensed designs.

The second factor is that PWI detectors are small; scene light is not directly collected by the photo detector in a PWI. Shot noise from the scene is the same as for the lens system. However, there is little dark current in a PWI design. The low dark current enables the possibility of a TE cooled, HgCdTe mid wave infrared imager.

The third factor in favor of PWI is that array uniformity is almost self-correcting. All LCS should indicate the same average signal strength, and that fact can be used to calibrate the array of photo detectors in-situ. In other words, the effect of variations in the optical couplers, waveguide splitters, and polarization diversifiers can be nulled along with detector variations.

7. Background on Silicon Waveguide Technology

This section provides background for the PWI implementation. Researchers in silicon waveguide fabrication have demonstrated the component parts needed to fabricate PWI. The various component parts can be mixed and matched to form practical FPA.

High efficiency air to silicon waveguide light couplers have been designed and fabricated. Figure 13 shows some examples of etched shapes; these pictures illustrate that fabricating couplers is well within state of the current art. Couplers that have been demonstrated include Bragg gratings, focused Bragg gratings, prism couplers, and tapered couplers, Coupling efficiencies from 0.1 to higher than 0.9 have been reported.

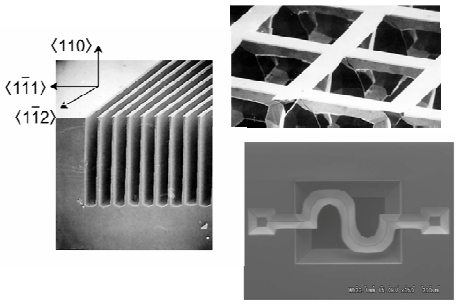

Figure 13. Some examples of anisotropic etching.

A typical silicon waveguide deposited on SiO_2 has a dimension of about 200 by 400 nanometers (nm). Researchers have found a way to make sharp turns without signal loss by making the corner a reflector. Researchers have also found ways to make efficient light distribution by using splitters and combiners. See Figure 14. When making complex waveguide networks, the waveguides can overlay each other without interaction if laid perpendicular.

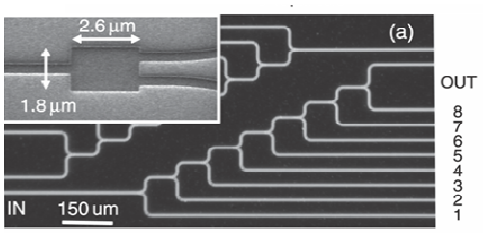

Figure 14. Waveguide light can be distributed efficiently.

Waveguides can be fabricated to favor TE modes, TM modes, or both. Further, polarization rotators have been designed. See Figure 15 for three examples that have been built and tested or their performance computer simulated. Situating waveguides to split TE and TM modes is also straightforward and efficient.

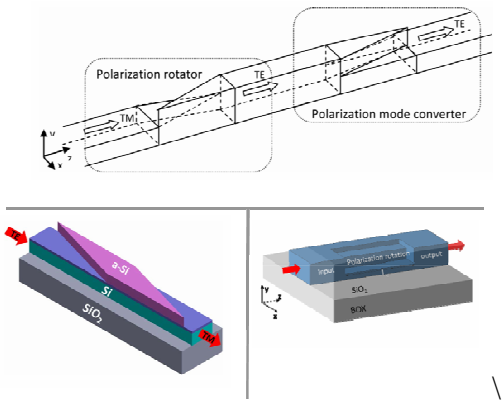

Figure 15. Three examples of polarization and mode converters.

Waveguide coupled germanium detectors with 60 giga-Hertz (GHz) bandwidth and 20 to 100 nanoamperes dark current have been demonstrated. However, the best overall combination of size and performance is a 1.3 by 4 micron detector with a 45 GHz bandwidth and 0.76 quantum efficiency with only 3 nanoamperes dark current.

Silicon waveguide technology has reached a high state of maturity, and the layout of, for example, one thousand by one thousand unit cells each 25 microns square is realistic. The waveguide themselves are small (200 by 400 nm, 400 nm by 200 nm, or 400 by 400 nm depending on mode or modes), corners can be sharp, waveguides can overlay each other without coupling, light coupling from air has been demonstrated and can be efficient, splitting and combining light is efficient, splitting polarization is efficient, and rotating the electric and magnetic fields has also been demonstrated with rotators as small as several microns.

8. Coupling Scene Light into the Waveguides

Coupling Concept 1

Both active and passive PWI require coupling scene light into waveguides. PWI have an innate signal to noise advantage, because the detectors are small and, in passive mode, speed is not required. Detector bias can be low, the detector area is small, and the dark current is therefore

minimal. Scene light coupling efficiencies on the order to 0.3 is more than sufficient for PWI performance to be competitive with conventional imaging.

However, that 0.3 efficiency factor includes both coupler fill factor and the ability of the coupler to impedance match the light from free-space to waveguide. The problem is not simple, and coupler development might be the major PWI development challenge. This section describes two possible approaches for fabricating coupler arrays.

The first coupler concept is illustrated in Figure 16. An actual wafer would have much smaller couplers and many more coupler arrays. Light enters through the back surface and the couplers are etched into the front surface. The coupler wafer is planarized. The photonics layer is fabricated separately and laid onto the couplers in the same manner as Silicon On Insulator fabrication.

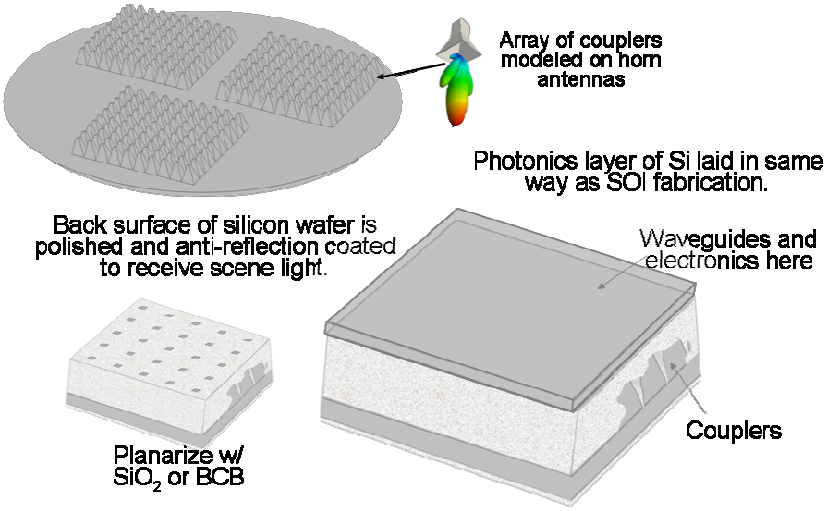

Figure 16. One concept of PWI layout and coupler fabrication.

Figure 17 shows more details of this first PWI layout concept. Other than the coupler array, all of the parts shown have been fabricated and tested by communications researchers.

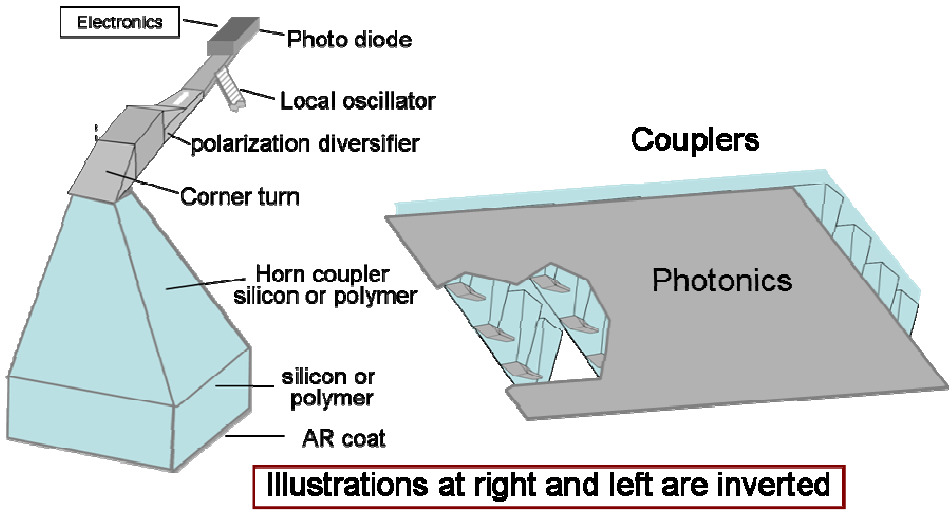

Figure 17 showing additional details of the first PWI layout.

Coupling efficiency is important for communications as well as imaging. However, researchers working on communications only need to couple one fiber optic in and one out. A lot more silicon area can be used, and the light is not collimated. Nonetheless, their experience provides the only available data.

The plot in Figure 18 summarizes efficiency data where researchers used a lens to focus 1.5 micron fiber optic light onto tapered couplers. It appears from their experience that a 200 micron taper length provides a little over 0.7 power coupling efficiency. That 0.7 factor is more than needed for good PWI operation, provided that the area fill factor is at least 0.5. The problem with achieving a high area fill factor is that it might make etching impractical.

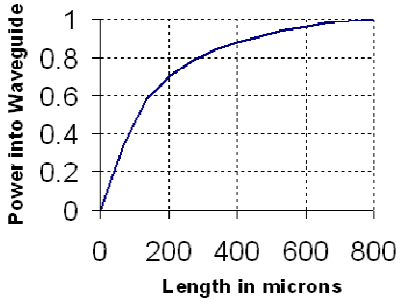

Figure 18. Plot of power coupling efficiency versus taper length. The wavelength used in the experiments was 1.5 microns.

Coupling Concept 2

A second possible approach is shown in Figure 19. With this approach, either amorphous silicon or polymer waveguides are laid down on top of the photonics circuit.

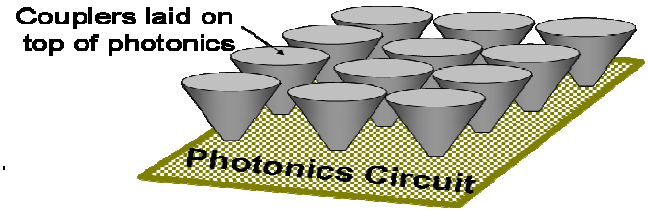

Figure 19. Either amorphous silicon or polymer couplers might be laid on top of the circuit.

In order to avoid sensitivity to side lobes, the J couplers or antenna horns are designed to reject light at angles greater than ± 1.49 degrees. (That specific angle derives from the choice of 1.3 micron wavelength and 25 micron unit cell pitch. See Equation 2.) Side lobe rejection is accomplished by the changing the angle of the converging slope of the horn in combination with the refractive indices of the coupler materials. The numerical aperture is purposely made small, and light at angles that would excite side lobes is rejected. The J couplers illustrated in Figure 11 are suggested as the primary unit cell implementation because they provide a means of rejecting off-axis light through the control of numerical aperture. Other implementations are certainly possible, and some of those possibilities are described below.

Note that, with PWI, sensitivity is related to receiver horn size and not cone angle. Small fields of view are implemented using large unit cell pitch, and that provides more room for the receive horns.

9. Limiting Off-Axis Light to Avoid Side-Lobes

Per Equation 2, PWI has side lobes. For small angles where cosine effects are small, the side-lobes have essentially the same sensitivity as the main lobe at normal incidence. With active operation, the scene is only illuminated in the main lobe. However, with passive operation, a way must be found to limit light outside the central field of view.

Horn antennas that limit side lobes have been designed in the RF and millimeter wave. Since our wavelengths are much smaller than LCS pitch, It is not clear why a proper horn cannot be etched into silicon or polymers. Other options exist, however.

One obvious solution is to use an afocal as shown in Figure 20. That solution defeats two of the advantages of PWI. First, a lens is required. Second, the image is now limited by aperture diffraction. However, in addition to restricting field of view, adding an afocal also improves resolution because of the afocal magnification. The afocal also provides flexibility in selecting field of view.

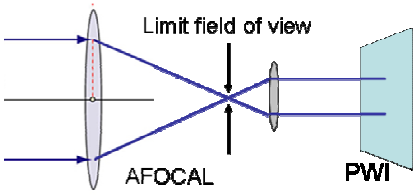

Figure 20. A PWI array could be incorporated into an afocal in order to control FOV.

Another option is to use narrow, multi-layer, dichroic spectral filters. These filters change wavelength transmission when tilted off-normal. By tilting two narrow spectral filters in front of the PWI, in-band light can only reach the PWI if it is at the correct angle. Figure 21 A illustrates filter placement and B illustrates filter behavior. A further option is to use volume Bragg gratings to control both field of view and wavelength.

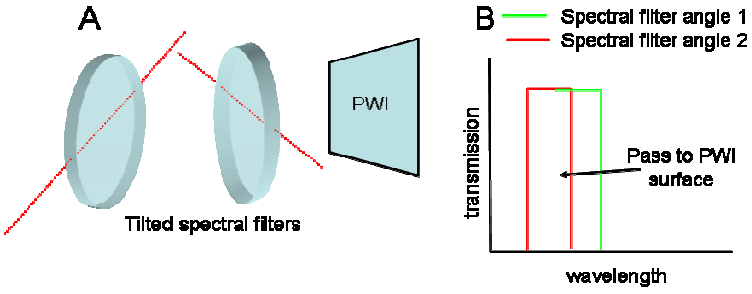

Figure 21. In A at left, two spectral filters are tilted in order to limit the angles at which light in the PWI spectral band can reach the PWI surface. In B at right, the tilted spectral filters have slightly different pass bands.

Other options include light pipes and lenslets. See Figure 22.

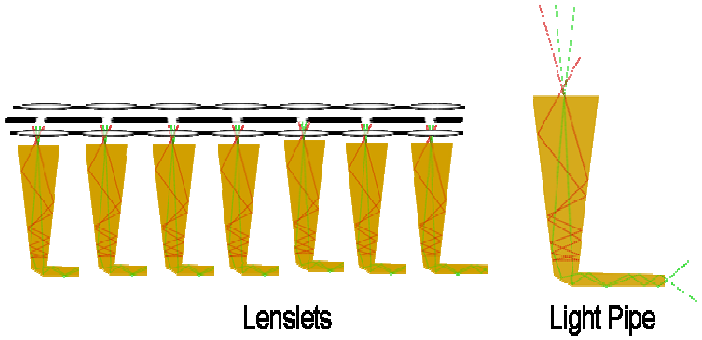

Figure 22. Either lenslets or light pipes might also be used to control side lobes.

10. Image Processing

Image data are collected by the light collection sites (LCS) as shown in Figure 8. The difference amplitudes in each LCS is corrected for gain variations by dividing by the sum of the photo diode signals in each LCS. A Fourier Transform of the PWI data creates the image.

11. Resolution Enhancement by Post-Processing Multiple PWI

The major PWI blur is caused by digital processing; that blur can be corrected by combining digital data from adjacent PWI. Figure 1 illustrates mounting a number of PWI in close proximity and using the combined signals to achieve improved signal to noise or better resolution or some combination of both. Resolution is enhanced by expanding the DFT. If the PWI are separated by distance D and PWI array positions are designated by (P,Q), then the Fourier Transform of the combined PWI sensors is given by Equation 16.

$$DFT_{all} = \sum_{P}\sum_{Q} DFT_{P,Q}\, e^{-i f_{PWI}^{x} PD}\, e^{-i f_{PWI}^{y} QD} \qquad (5)$$

where $DFT_{P,Q}$ represents the DFT data at position (P,Q) and DFT_{all} is the data for the final discrete transform. Equation 16 assumes that all of the PWI are precisely aligned or that the relative alignment is accurately measured and individual DFT phases adjusted accordingly.

If the precise alignment between individual PWI is not known, then cross-correlating the individual images provides offset tilt information. The individual images are brought into coincidence by using digital processing to register the multiple images of the same scene to within a fraction of a pixel.

Once the individual images are properly aligned in angle space, the pixels representing the overlapped field of view are inverse transformed. Notice that field of view has been lost due to the tilt errors. In the Frequency Domain, the tilt offset information is used to transform all DFT data into the same coordinate system. The new individual $DFT_{P,Q}$ are then used to find DFT_{all}.

If signal to noise improvement is desired, then signal to noise increases by the square root of the number of PWI images summed. If desired, some images can be summed to improve signal to noise and other images used to expand the DFT to improve resolution.